Cancer Cell
Article

# Expression of Mutant p53 Proteins Implicates a Lineage Relationship between Neural Stem Cells and Malignant Astrocytic Glioma in a Murine Model

Yuan Wang,[1,2,6] Jiong Yang,[1,2,6] Huarui Zheng,[1,2] Gerald J. Tomasek,[1,2] Peng Zhang,[1,2] Paul E. McKeever,[3] Eva Y.-H.P. Lee,[4,5] and Yuan Zhu[1,2,*]
[1]Division of Molecular Medicine and Genetics, Department of Internal Medicine
[2]Department of Cell and Developmental Biology
[3]Department of Pathology
University of Michigan Medical School, Ann Arbor, MI 48109, USA
[4]Department of Developmental and Cell Biology
[5]Department of Biological Chemistry
University of California, Irvine, Irvine, CA 92697, USA
[6]These authors contributed equally to this work
*Correspondence: yuanzhu@umich.edu
DOI 10.1016/j.ccr.2009.04.001

## SUMMARY

**Recent studies have identified genes and core pathways that are altered in human glioblastoma. However, the mechanisms by which alterations of these glioblastoma genes singly and cooperatively transform brain cells remain poorly understood. Further, the cell of origin of glioblastoma is largely elusive. By targeting a *p53* in-frame deletion mutation to the brain, we show that p53 deficiency provides no significant growth advantage to adult brain cells, but appears to induce pleiotropic accumulation of cooperative oncogenic alterations driving gliomagenesis. Our data show that accumulation of a detectable level of mutant p53 proteins occurs first in neural stem cells in the subventricular zone (SVZ) and that subsequent expansion of mutant p53-expressing Olig2$^+$ transit-amplifying progenitor-like cells in the SVZ-associated areas initiates glioma formation.**

## INTRODUCTION

Glioblastoma (grade IV malignant astrocytic glioma), also known as glioblastoma multiforme (GBM), is the most frequent and aggressive neoplasm among human primary brain tumors (Furnari et al., 2007; Louis et al., 2007). There are two subtypes of GBM. Primary GBM arises de novo with no evidence of preexisting lesions, whereas secondary GBM develops from lower-grade, albeit malignant (i.e., grade II or III) gliomas. Despite distinctive clinical courses and differing molecular lesions, primary and secondary GBMs share the same histopathological and clinical features, most notably a high propensity to diffusely infiltrate normal brain parenchyma and resistance to virtually all current therapies. Consequently, GBM is one of the most deadly human cancers with a median survival that has remained at 12 months for over the past two decades (Furnari et al., 2007; Louis et al., 2007).

Recent studies have identified genes and core pathways that are altered in human GBM (Ohgaki et al., 2004; Parsons et al., 2008; Cancer Genome Atlas Research Network, 2008). Mutations in the components of the TP53 tumor suppressor pathway have been identified in the majority of human primary GBM, approximately 30% to 40% of which have mutations in the *TP53* gene (Parsons et al., 2008; Cancer Genome Atlas Research Network, 2008). Furthermore, frequencies of *TP53* mutations are high and similar among lower-grade malignant

## SIGNIFICANCE

Glioblastoma is the most malignant form of astrocytic gliomas and the most common primary brain cancer in adults. The poor prognosis of glioblastoma emphasizes the urgent need for a greater understanding of disease pathogenesis. We demonstrate that p53 deficiency can cooperate with diverse mitogenic signaling pathways to induce malignant glioma. For example, inactivation of the *Nf1* tumor suppressor, activation of mitogen-activated protein kinase, or activation of phosphatidylinositol-3-OH kinase pathways are not essential, but can promote p53-mediated glioma formation. Furthermore, expression of mutant p53 proteins is identified as a marker for glioma cells in all stages. Analysis of brain cells with a detectable level of mutant p53 expression provides important insights into the role of neural stem cells and transit-amplifying progenitors in p53-mediated gliomagenesis.

gliomas and secondary GBMs, suggesting an important role of *TP53* gene defects in early stages of glioma development (Ohgaki et al., 2004). Consistently, individuals with Li-Fraumeni syndrome, who carry germline *TP53* mutations, are predisposed to development of astrocytic gliomas (Louis et al., 2007). However, the mechanisms by which TP53 deficiency transforms normal brain cells remain poorly understood.

One critical challenge to understand the GBM pathogenesis is to identify the cell of origin of this disease. The cell of origin in most human cancers remains unknown as human tumors are typically presented at the terminal stages of the disease and thus do not provide a window to study this important question. Recent studies demonstrated that a number of brain cancers, including GBM, are driven and sustained by a subset of stem cell-like cells that exhibit the cellular characteristics of normal stem cells, including self-renewal and multipotency (Galli et al., 2004; Hemmati et al., 2003; Singh et al., 2004). However, whether a normal stem cell, a progenitor cell, or even a fully differentiated cell is the cell of origin for glioma stem cells remains largely unknown (Sanai et al., 2005; Stiles and Rowitch, 2008). In the adult brain, multipotent neural stem and progenitor cells are spatially restricted in two stem cell niches: the subventricular zone (SVZ) of the lateral ventricle and the subgranular zone of the hippocampal dentate gyrus (Merkle and Alvarez-Buylla, 2006). Genetic studies using murine glioma models and imaging analysis from a clinical study provide evidence that some GBMs may arise from the SVZ stem cell niche (Alcantara Llaguno et al., 2009; Lim et al., 2007; Zhu et al., 2005a). At the cellular level, neural stem cells in the adult SVZ (type B cells or SVZ-B) give rise to a highly proliferative cell population, transit-amplifying progenitor cells (SVZ-C cells), which then differentiate into two lineage-restricted progenitor cells, neuroblasts (SVZ-A cells) and oligodendrocyte precursor cells (SVZ-OPC) (Hack et al., 2005; Menn et al., 2006). Because of a lack of reliable markers for glioma cells, particularly at early stages of tumor development, the role of the various SVZ cell populations in gliomagenesis remains undefined.

In this study, we develop a murine glioma model in which an in-frame *p53* deletion mutation is specifically targeted into the nervous system and use it to investigate the role of neural stem cells and transit-amplifying progenitors in p53-mediated gliomagenesis.

## RESULTS

### Neural-Specific p53 Targeting Strategy

To investigate the role of *p53* in gliomagenesis, we used two transgenic mouse strains to target a *p53* mutation into the nervous system. The first one expresses Cre under the control of the human glial fibrillary acidic protein (GFAP) promoter (hereafter, hGFAP-cre). The hGFAP-cre transgene is specifically expressed in radial glial cells during embryonic development and in mature astrocytes of the postnatal brain (Malatesta et al., 2003; Zhuo et al., 2001). Because radial glial cells are the primary multipotent neural stem/progenitor cell populations in the developing brain, hGFAP-cre-mediated gene deletion will be transmitted to all the progeny of radial glial cells, including neurons, glia, and adult neural stem cells (Merkle and Alvarez-Buylla, 2006). Thus, the hGFAP-cre-mediated neural-specific gene inactivation permits assessment of the relative tumor susceptibility or ''tumor competence'' of neural stem cells, progenitor cells, and mature glia in the adult brain (see Figure S1 available online). The second strain harbors a *p53* conditional allele (*p53*flox) (Lin et al., 2004). Cre-mediated recombination of this *p53*flox allele results in an in-frame deletion of exons 5 and 6 (Figure 1A), which encode a significant portion of the p53 DNA binding domain (Cho et al., 1994; Kitayner et al., 2006). Consistently, it has been previously shown that this *p53* in-frame deletion mutant (hereafter, $p53^{\Delta E5\text{-}6}$) lacks transcriptional function (Lin et al., 2004). Thus, the $p53^{\Delta E5\text{-}6}$ allele represents a DNA binding domain-deficient loss-of-function allele.

### p53 Deficiency Drives Tumor Formation in the Adult Brain

To study tumorigenic activity of the $p53^{\Delta E5\text{-}6}$ mutation in the brain, we crossed the hGFAP-cre line with the *p53*flox mouse to generate hGFAP-cre+;$p53^{flox/+}$ mice. We monitored ten hGFAP-cre+;$p53^{flox/+}$ mice over 12 months. These mice were healthy and behaved indistinguishably from the wild-type littermates. Moreover, we found no evidence of tumor formation in the brain of these aged mice (data not shown). We then generated hGFAP-cre+;$p53^{flox/KO}$ (hereafter referred to as conditional knockout 1 or CKO1) and hGFAP-cre+;$p53^{flox/flox}$ (CKO2) mouse strains (Figure 1B). As we have previously shown that inactivation of *p53* followed by *Nf1* loss efficiently induces malignant gliomas with complete penetrance (Zhu et al., 2005a), we introduced a heterozygous *Nf1* mutation to the $p53^{\Delta E5\text{-}6}$ mutant background and generated a third mutant strain with the genotype of hGFAP-cre+;$p53^{flox/flox}$;$Nf1^{KO/+}$ (CKO3). In CKO3 brains, p53-deficient cells are expected to inactivate the *Nf1* wild-type allele to undergo *p53*/*Nf1*-mediated gliomagenesis, whereas p53-deficient cells in the CKO1/2 brains could potentially cooperate with diverse oncogenic alterations to drive glioma formation (Figure 1B).

Both CKO1 and CKO2 mice were healthy, fertile, and indistinguishable from their control littermates within the first 6 months after birth (Figure 1C). However, 85% of CKO1 (22/26) and 84% of CKO2 (43/51) mice analyzed in this study developed neurological symptoms including tremor, seizure, ataxia, or lack of balance requiring sacrifice between the ages of 6 and 14 months (Figure 1C). Each of the CKO1 and CKO2 mice with neurological deficits exhibited enlarged brains with evidence of high-grade brain tumors. The remaining CKO1 and CKO2 mice were sacrificed because of the presence of tumors outside the central nervous system (CNS). These non-CNS tumors were diagnosed as soft-tissue sarcomas, likely arising due to hGFAP-cre expression in cells outside the CNS (data not shown). A portion of the CKO1 (1/4) and CKO2 (2/8) mice with non-CNS sarcomas also exhibited enlarged brains with high-grade tumors. Together, nearly 90% of both CKO1 (23/26) and CKO2 (45/51) mutant mice developed high-grade brain tumors (Figure 1B), most of which (20/23 of CKO1 and 40/45 of CKO2) were histopathologically characterized as malignant gliomas with astrocytic characteristics and the remainder of which were medulloblastomas (Figure 1D). Because CKO1 and CKO2 mice exhibited essentially the same brain tumor phenotypes (Figures 1B–1D), they will be presented together as the $p53^{\Delta E5\text{-}6}$ mutant mice.

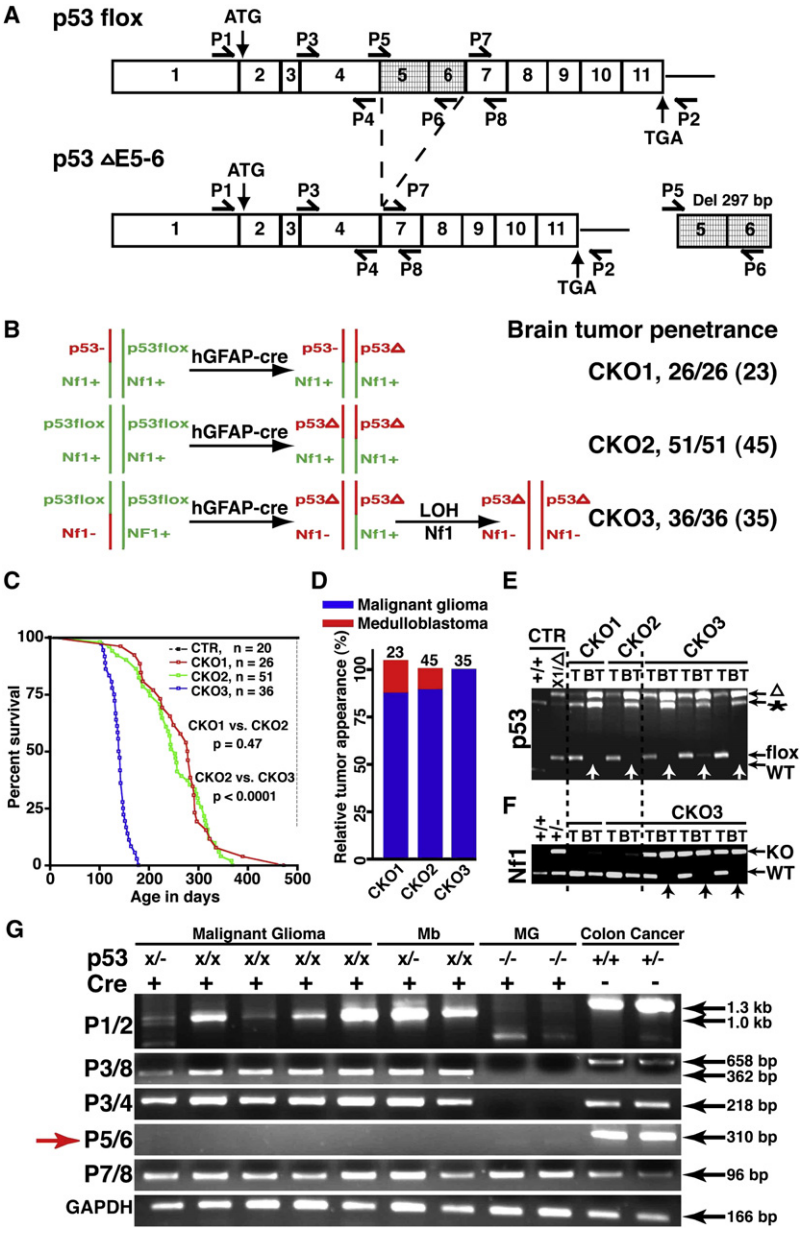


**Figure 1. Construction and Characterization of the CKO1, CKO2, and CKO3 Mice**

(A) The exon structure of the *p53*flox and deleted $p53^{\Delta E5\text{-}6}$ (Del) alleles and RT-PCR strategy. Positions for the primers (P1–P8) are illustrated.

(B) Schematic drawing of the genetic configurations of CKO1–3 mice. All the mutant mice analyzed developed brain tumors, including those in early stages. The number in parentheses shows the number of mutant mice that developed high-grade brain tumors.

(C) Survival curves of control and CKO1–3 mutant mice. p value was obtained from Kaplan-Meier survival test.

(D) The percentage of malignant astrocytic gliomas and medulloblastomas observed in the mutant mice with high-grade brain tumors. Of note, 1 of 23 CKO1 mice developed both malignant glioma and medulloblastoma.

(E and F) Genomic DNAs isolated from the tails (T) and brain tumors (BT, arrows) of CKO1–3 mice were subjected to PCR analysis for the *p53* (E) and *Nf1* (F) alleles. WT, wild-type allele; flox, *p53*flox allele; (*), *p53* pseudogene; Δ, deleted *p53* allele; KO, *Nf1* knockout allele.

(G) RT-PCR analysis showing an aberrant transcript, lacking exons 5 and 6, produced from the mutant alleles in brain tumors including malignant glioma and medulloblastoma (Mb). The *p53* full-length cDNAs were amplified from colon cancers of the $Smad3^{-/-}$ mice, serving as a positive control; the *p53* null cDNAs from malignant gliomas (MG) of the hGFAP-cre+;$p53^{KO/KO}$;$Nf1^{flox/flox}$ mice were used as a negative control. Of note, the *p53* null allele produces a truncated transcript lacking exons 1–6.

## Mutant $p53^{\Delta E5\text{-}6}$ Expression Marks p53-Deficient Brain Tumor Cells

To determine whether Cre-mediated *p53* deletion drives tumor formation, we first performed PCR analysis on genomic DNA of brain tumors isolated from $p53^{\Delta E5\text{-}6}$ mutant mice (n = 6) and found that the *p53*flox allele had been completely converted to the $p53^{\Delta E5\text{-}6}$ allele (Figure 1E). RT-PCR analysis revealed that the $p53^{\Delta E5\text{-}6}$ transcript was the only *p53* transcript that could be detected in these tumors (n = 7) (Figure 1G). We further cloned and sequenced the *p53* cDNAs and genomic DNAs derived from these brain tumors and found no somatic mutation other than the expected deletion of exons 5 and 6 (see Experimental Procedures). Similar to human tumors, all the $p53^{\Delta E5\text{-}6}$ brain tumors expressed high levels of mutant p53 proteins (Figures 2A–2F and Figures 3Cb and 3Cb′). The p53 nuclear immunostaining was very specific for $p53^{\Delta E5\text{-}6}$ brain tumor cells, as no labeling was observed in the normal brain cells, including those carrying one or two $p53^{\Delta E5\text{-}6}$ alleles, or in the p53 null malignant astrocytic gliomas (Table S1) (Zhu et al., 2005a). In addition, we crossed the $p53^{\Delta E5\text{-}6}$ mutant mice (CKO1 and CKO2) to a mouse strain harboring the Rosa26-LacZ reporter (R26R-LacZ), whose expression requires Cre-mediated recombination (Soriano, 1999). Nearly all the SVZ stem and progenitor cells as well as Olig2-expressing progenitors and oligodendrocytes in the corpus callosum of the resulting mice could readily be labeled by β-galactosidase (β-gal) expressed from the R26R-LacZ (Figures S1B and S1C). Accordingly, all the $p53^{\Delta E5\text{-}6}$ brain tumors analyzed extensively expressed high levels of β-gal (Figures 2Ga and 2Ga′). Furthermore, almost all the $p53^{\Delta E5\text{-}6}$-positive brain tumor cells exhibited high levels of β-gal expression (Figures 2Gb and 2Gb′). It is worth noting that three of five $p53^{\Delta E5\text{-}6}$ brain tumors analyzed contained a subpopulation of tumor cells with no or low β-gal staining, which often exhibited high levels of GFAP and hGFAP-cre expression (Figure 2H and data not shown). This is consistent with the previous observations that the R26R-LacZ is not expressed in most GFAP-expressing mature astrocytes, despite their expression of hGFAP-cre (Figure S1C) (Malatesta et al., 2003). Taken together, these studies demonstrate that brain tumors observed in this model arose from p53-deficient cells, which can be specifically marked by a detectable mutant p53 protein expression.

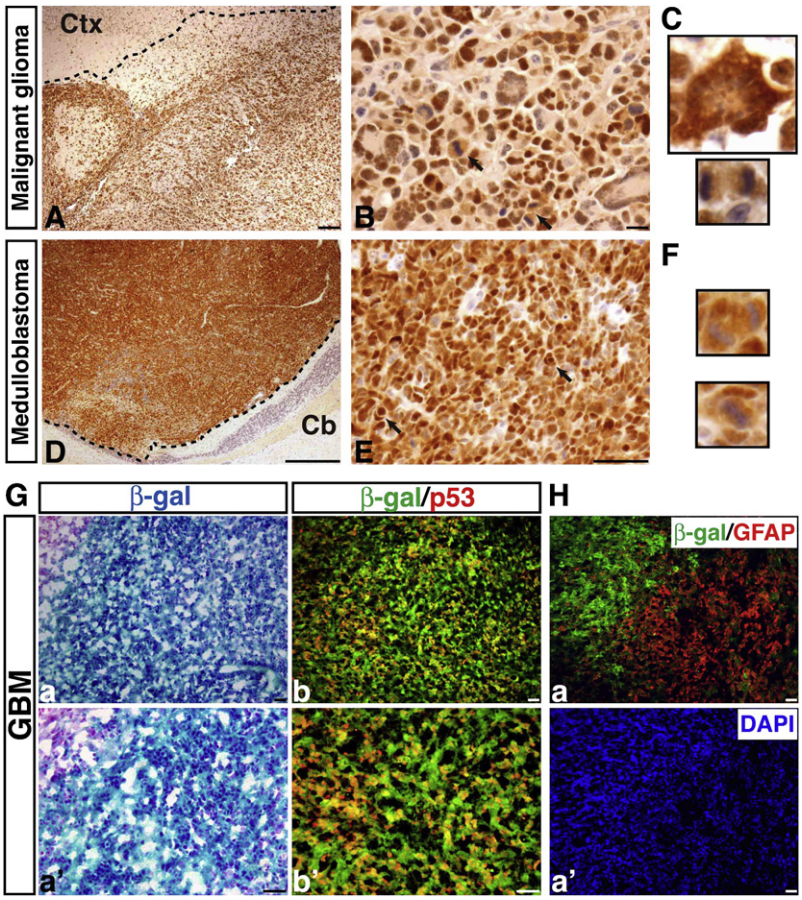


**Figure 2. P53$^{\Delta E5\text{-}6}$ Brain Tumors Specifically Express a Detectable Level of Mutant p53 Proteins**

Representative examples showing p53$^{\Delta E5\text{-}6}$-positive malignant astrocytic gliomas (A and B) and medulloblastomas (D and E). The dashed lines roughly mark the border of the tumors and surrounding brain tissues because of the infiltrating nature of these tumors (A and D). Arrows in (B) and (E) point to mitotic figures in malignant gliomas and nuclear molding in medulloblastomas, respectively.

(C) High magnification views of a p53$^{\Delta E5\text{-}6}$-positive multinucleated giant cell (top) and mitotic figure (bottom) in a malignant glioma.

(F) High magnification views of a p53$^{\Delta E5\text{-}6}$-positive mitotic figure (top) and nuclear molding (bottom) in a medulloblastoma. Ctx, cerebral cortex; Cb, cerebellum.

(G) Adjacent sections from p53$^{\Delta E5\text{-}6}$ brain tumors harboring the R26R-LacZ transgene were stained with X-gal (a and a′) and anti-β-gal/anti-p53 antibodies (b and b′). All the p53$^{\Delta E5\text{-}6}$-positive tumor cells exhibited β-gal expression, indicating p53 deficiency.

(H) A small population of tumor cells expressed little or no β-gal, but had high levels of GFAP expression (a). Tumor nuclei were counterstained with DAPI (a′). Scale bars, 50 μm.

## CD133$^{+}$ Malignant Astrocytic Glioma and GBM

Malignant astrocytic gliomas observed in the advanced-stage p53$^{\Delta E5\text{-}6}$ mice diffusely infiltrated the forebrain and expressed glioma markers GFAP, Nestin, and Olig2, albeit with a high degree of heterogeneity within individual tumors and between different tumors (Figures 3A and 3B and Figure S2 and Table S2). Importantly, approximately 40% of the p53$^{\Delta E5\text{-}6}$ high-grade astrocytic gliomas exhibited the characteristics of human GBM, including the presence of necrosis, pseudopalisading tumor cells, and microvascular proliferation (Figure 3A). It is worth noting that regardless of the presence or absence of detectable necrosis, these malignant gliomas exhibited similarly high degrees of nuclear atypia (Figure 3B and Figures S2B and S3), resembling human primary GBM. These tumors also exhibited the defining features of human high-grade diffuse gliomas: high levels of mitotic figures and presence of secondary structures of Scherer (Figures 2B and 3C). Furthermore, similar to human counterparts, a subpopulation of p53$^{\Delta E5\text{-}6}$ tumor cells expressed a glioma stem cell marker, CD133 (also known as prominin1), and the CD133$^{+}$ glioma cells were often located around blood vessels and expressed p53, Nestin, and Olig2 (Figure S4) (Calabrese et al., 2007; Singh et al., 2004). Taken together, the p53$^{\Delta E5\text{-}6}$ mouse model accurately recapitulates both the genetics and pathology of human high-grade astrocytic gliomas.

## p53 Deficiency Provides No Significant Growth Advantage to Adult Brain Cells

To investigate the mechanisms underlying p53-mediated gliomagenesis, we examined the brain of young adult mutant mice. At 2 months of age, no significant difference was identified between the control and p53$^{\Delta E5\text{-}6}$ brains (n = 6 for each genotype), which is consistent with the notion that p53 is dispensable for normal brain development (Donehower et al., 1992; Jacks et al., 1994). Although previous studies demonstrated that a germline p53 null mutation results in mild hyperplasia in the SVZ of the adult brain (Gil-Perotin et al., 2006; Meletis et al., 2006), we found no abnormality in the p53$^{\Delta E5\text{-}6}$ mutant SVZ stem cell niche with respect to the number or the density of the total SVZ cells (Figure S5). Furthermore, no significant difference in the number, the density, or the percentage of BrdU-positive proliferating cells was identified between the control and mutant brains including the SVZ region at 2 months (Figures S5M–S5Q). Together, these results indicate that the *p53*$^{\Delta E5\text{-}6}$ mutation does not confer a measurable growth advantage to brain cells including SVZ stem and progenitor cells in young adult mice.

## P53 Deficiency Induces Accumulation of Cooperative Oncogenic Events

The results described above suggest that additional cooperative oncogenic alterations must occur to transform p53-deficient brain cells. To test this, we examined the status of other GBM core pathways such as Rb and receptor tyrosine kinase (RTK) signaling pathways in these tumors. Western blot analysis revealed that all the p53$^{\Delta E5\text{-}6}$ gliomas exhibited high levels of Cdk4 expression and about half of the tumors also had cyclin D1 overexpression, whereas the expression of Rb and p27 was not significantly different between tumors and control

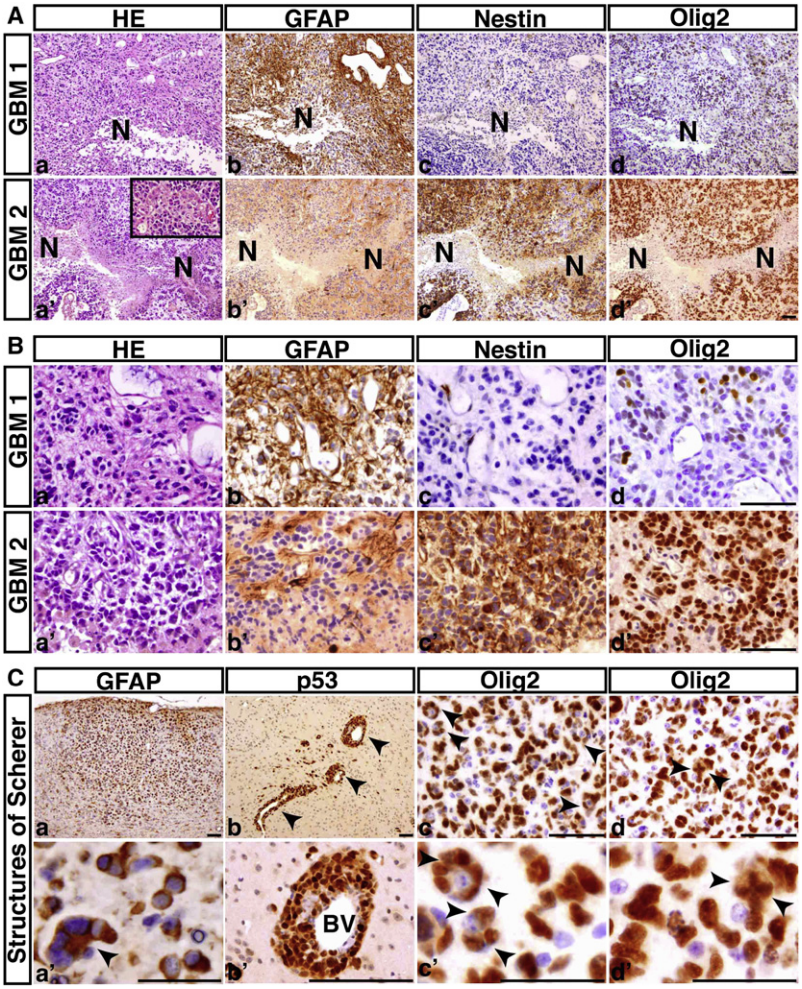


**Figure 3. The p53$^{\Delta E5\text{-}6}$ Mutant Mice Develop GBMs**

(A) Serial sections from two representative p53$^{\Delta E5\text{-}6}$ GBMs (GBM1 and GBM2) were stained with H&E (a and a′), anti-GFAP (b and b′), anti-Nestin (c and c′), and anti-Olig2 (d and d′). N, necrosis. There are regions of coagulation necrosis (a–d) and pseudopalisades of malignant GBM cells adjacent to necrosis (a′–d′). The inset in (a′) shows microvascular proliferation in this GBM.

(B) High-magnification views of (A) illustrate that both malignant cells and nuclei are highly pleomorphic. Many GBM cells have substantial cytoplasm and some have eccentric nuclei (a and a′).

(C) The p53$^{\Delta E5\text{-}6}$ gliomas exhibit the secondary structures of Scherer: accumulation of GFAP-positive tumor cells in the subpial zone of the cerebral cortex (a and a′); perivascular satellitosis (b and b′, arrowheads); and perineuronal satellitosis (c and c′, arrowheads). (d and d′) The examples of Olig2$^{+}$ tumor cells with abnormal mitoses (arrowheads). BV, blood vessels. Scale bars: (A, B, and Ca–Cd), 50 μm; (Ca′–Cd′), 25 μm.

forebrains (Figure 4A). Moreover, some tumors accumulated high levels of p16 and p21 in a mutually exclusive manner. These results demonstrate that deregulation of the Rb-mediated cell cycle regulatory pathway is a universal phenomenon in these p53$^{\Delta E5\text{-}6}$ gliomas. Because deregulation of one of the RTKs, platelet-derived growth factor receptor (PDGFR), is often identified in human malignant gliomas with *TP53* mutations (Furnari et al., 2007; Louis et al., 2007), we investigated the expression of PDGFRα and its ligands in the p53$^{\Delta E5\text{-}6}$ gliomas. Compared to normal brains, all the p53$^{\Delta E5\text{-}6}$ gliomas analyzed in this study exhibited high levels of expression of PDGFRα and its two ligands, PDGF-A and PDGF-B (Figure 4B), suggesting that these tumor cells established an autocrine or paracrine stimulatory loop of the PDGF/PDGFR signaling. As in human tumors (Furnari et al., 2007), the p53$^{\Delta E5\text{-}6}$ malignant astrocytic gliomas at all stages analyzed (n = 8) exhibited high levels of PDGFRα expression (Figure S3), suggesting that activation of PDGFR signaling is an early event in p53-mediated gliomagenesis.

We then investigated two mitogenic signaling pathways, the phosphatidylinositol-3-OH kinase (PI3K) and mitogen-activated protein kinase (MAPK), which are major effectors of RTK signaling. The expression of a major negative regulator of the PI3K pathway, the *Pten* tumor suppressor, was either lost or significantly reduced in over 80% of the p53$^{\Delta E5\text{-}6}$ gliomas (Figure 4B). Consistently, the majority of the p53$^{\Delta E5\text{-}6}$ gliomas exhibited activation of the PI3K signaling pathway evidenced by increased levels of phosphorylated Akt (Figure 4B and Figures S6A–S6L). As a negative regulator of Ras oncoprotein, *NF1* tumor suppressor gene was previously found overexpressed in human sporadic GBMs (Gutmann et al., 1996). Consistently, compared to normal brains, most p53$^{\Delta E5\text{-}6}$ gliomas exhibited increased expression of Nf1 (Figure 4B). However, one of seven (14%) p53$^{\Delta E5\text{-}6}$ gliomas analyzed exhibited loss of Nf1 expression, which agreed well with more recent large-scale genomic studies that *NF1* is mutated in approximately 15% of human GBMs (Parsons et al., 2008; Cancer Genome Atlas Research Network, 2008). Accordingly, only half of the p53$^{\Delta E5\text{-}6}$ gliomas exhibited activation of the MAPK signaling pathway (Figures 4B–K). Together, these results indicate that the p53$^{\Delta E5\text{-}6}$ mutation can induce accumulation of downstream oncogenic alterations in Rb and RTK signaling pathways, which drive gliomagenesis. Importantly, these results validate molecular fidelity of the p53$^{\Delta E5\text{-}6}$ model to human GBM.

## *Nf1* Inactivation Promotes p53-Mediated Malignant Glioma Formation

Despite that *Nf1* inactivation, activation of PI3K or MAPK signaling pathways appears not essential for p53-mediated gliomagenesis; all the CKO3 mice (hereafter, *p53*$^{\Delta E5\text{-}6}$;*Nf1*$^{-/-}$) analyzed (n = 36) developed malignant astrocytic gliomas with significantly shorter latency compared to the p53$^{\Delta E5\text{-}6}$ mutant mice (Figures 1B–1D). Strikingly, nearly 70% of malignant gliomas observed in *p53*$^{\Delta E5\text{-}6}$;*Nf1*$^{-/-}$ mice exhibited histopathological features of human GBM, such as necrosis (Figure S7). Molecular analysis confirmed that *p53*$^{\Delta E5\text{-}6}$;*Nf1*$^{-/-}$ gliomas arose from *p53* (Figure 1E) and *Nf1* double deficient cells, as evidenced by invariable loss of the *Nf1* wild-type allele (Figure 1F, arrows). Compared to the p53$^{\Delta E5\text{-}6}$ gliomas, the

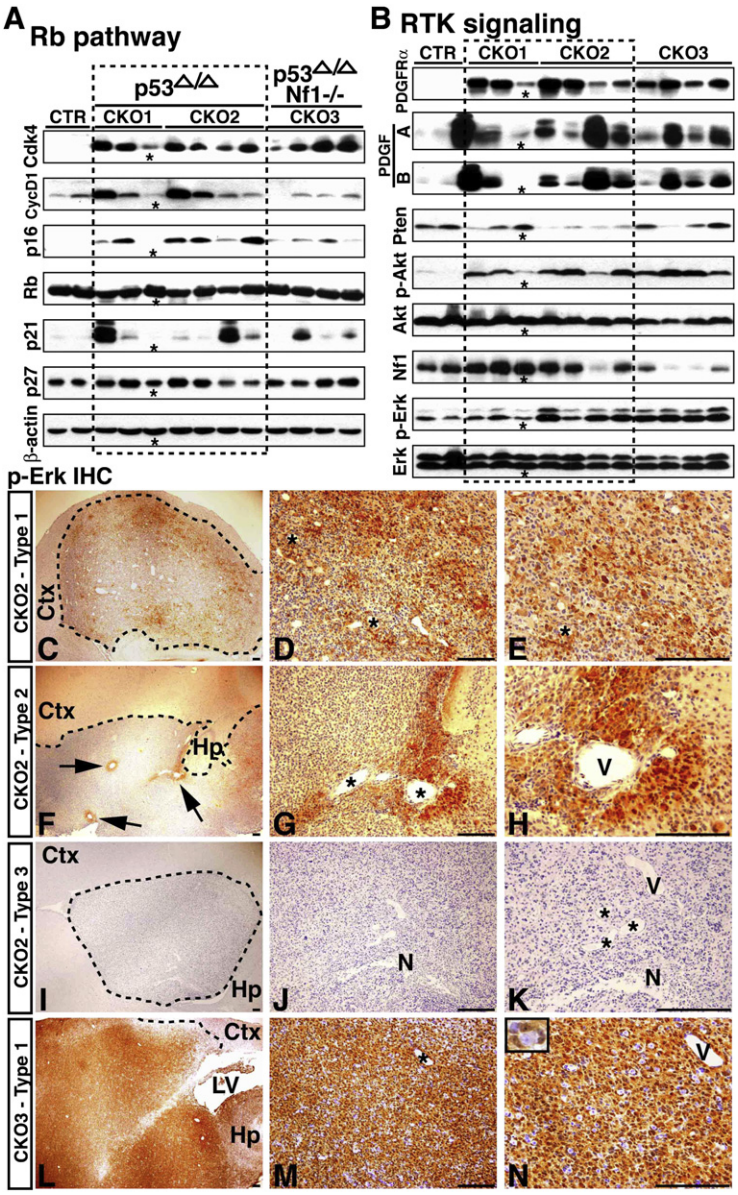


**Figure 4. Molecular Characterization of Malignant Astrocytic Gliomas**

(A) Western blot analysis of the Rb pathway. Protein extracts from normal forebrain tissues, $p53^{\Delta E5\text{-}6}$ gliomas (CKO1 and CKO2), and $p53^{\Delta E5\text{-}6}$;$Nf1^{-/-}$ gliomas (CKO3) were analyzed by western blot analysis using antibodies against components in the G1/S cell cycle regulatory circuits. β-actin was used as a loading control.

(B) Western blot analysis of the RTK and mitogenic signaling pathways on the same samples analyzed in (A). A glioma sample marked by an asterisk was found contaminated with a significant amount of normal tissues.

(C–N) Sections of malignant gliomas marked by dashed lines from CKO2 (C–K) and CKO3 (L–N) mice were stained with an anti-p-Erk antibody. Based on the number and pattern of p-Erk-positive cells, the $p53^{\Delta E5\text{-}6}$ gliomas are highly heterogeneous and can be classified into three types: (1) Type 1 tumors have extensive p-Erk staining (C–E), (2) Type 2 tumors only have a small number of p-Erk-positive cells that are typically found associated with blood vessels (F–H), and (3) Type 3 tumors exhibit no p-Erk staining (I–K). N in (J) and (K) labels necrosis. In contrast, the $p53^{\Delta E5\text{-}6}$;$Nf1^{-/-}$ gliomas are relatively homogeneous and exhibit extensive and intense p-Erk staining (L–N). Ctx, cerebral cortex; Hp, hippocampus; LV, lateral ventricle; V and *, blood vessels. The inset in (N) shows an example of p-Erk-positive cells encircling a neuron. Scale bars, 100 μm.

$p53^{\Delta E5\text{-}6}$;$Nf1^{-/-}$ gliomas exhibited relatively similar molecular alterations between individual tumors as well as in cells within a tumor. For example, all the $p53^{\Delta E5\text{-}6}$;$Nf1^{-/-}$ gliomas exhibited consistent activation of MAPK and PI3K/Akt pathways (Figures 4B and 4L–4N and Figures S6M–S6R). At histopathological levels, unlike the $p53^{\Delta E5\text{-}6}$ tumors, the $p53^{\Delta E5\text{-}6}$;$Nf1^{-/-}$ gliomas exhibited a relatively homogeneous expression pattern of lineage markers (Figure S7 and Table S2). Thus, these results demonstrate that *Nf1* inactivation, as one of the cooperative oncogenic alterations, albeit not essential, can rapidly promote $p53^{\Delta E5\text{-}6}$-mediated gliomagenesis.

## Expression of Mutant $p53^{\Delta E5\text{-}6}$ Proteins Marks the Earliest-Stage Glioma Cells

The molecular and histological studies of $p53^{\Delta E5\text{-}6}$ and $p53^{\Delta E5\text{-}6}$;$Nf1^{-/-}$ gliomas suggest that acquired cooperative oncogenic alterations can influence the histological features of advanced-stage malignant gliomas. Alternatively, the high histological heterogeneity of $p53^{\Delta E5\text{-}6}$ malignant gliomas could result from distinct cell(s) of origin. To distinguish these two possibilities, we first sought to identify the putative earliest-stage glioma cells (for simplicity, referred to as glioma precursor). In the normal adult brain, particularly after 4 months of age, virtually all the proliferating cells are restricted to the SVZ or RMS (Figure 5A). This extremely low proliferation background permits the use of BrdU immunostaining as a sensitive assay to identify glioma precursors. Based on the time course of tumor development in $p53^{\Delta E5\text{-}6}$ mice (Figure 1C), we studied the brain of 10 mutant mice at ages of 4 to 4.5 months and found that all of them exhibited abnormal proliferation in the portion of the corpus callosum immediately adjacent to the SVZ or RMS (Figures 5B and 5C). Specifically, four of these ten $p53^{\Delta E5\text{-}6}$ brains had small clusters of abnormal proliferating cells, three of which were identified in the corpus callosum immediately adjacent to the SVZ (Figures 5B′ and 5C′) and one was observed in the olfactory bulb (OB) (see Figure 8D). By analyzing the serial sections of these four brains, we confirmed that the identified proliferating clusters were the only proliferating cell clusters present in these brains. Thus, these results indicate that the proliferating clusters constitute the initially expanding glioma precursors. Consistently, many cells in the proliferating cell clusters exhibited a high degree of nuclear atypia (Figures 5D and 5F, arrows), a property reminiscent of malignant glioma cells. In addition to the cells in the adult neurogenic niches, glioma precursors were the only cells in mutant brains that expressed Nestin, which is never found in the normal corpus callosum (Figures 5E and 5G, top panels). Together, we conclude that glioma precursors in most mutant brains were Nestin-expressing ($Nestin^{+}$) cells located in the corpus callosum immediately adjacent to the SVZ.

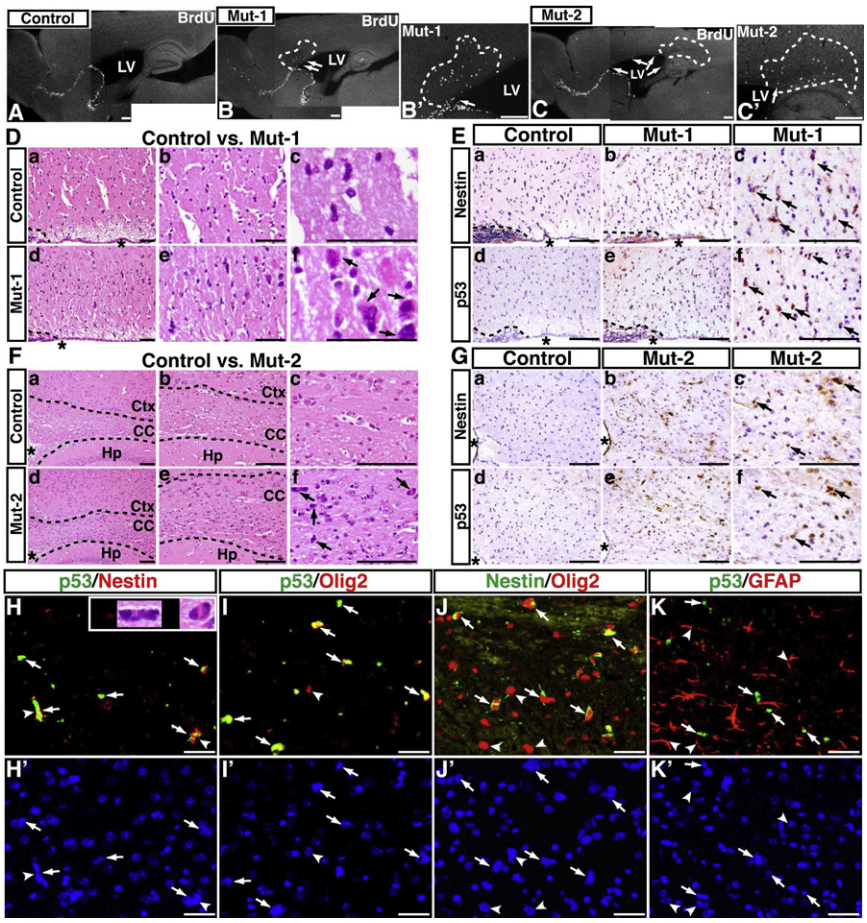


**Figure 5. Expression of Mutant p53$^{\Delta E5\text{-}6}$ Proteins Identifies the Earliest-Stage Glioma Cells**

(A–C) BrdU staining was performed on sections from age-matched control (A) and two representative p53$^{\Delta E5\text{-}6}$ brains that contain proliferation clusters (marked by dashed lines) in the corpus callosum adjacent to the anterior SVZ (B and B′, Mut-1) and to the posterior SVZ (C and C′, Mut-2), respectively. Arrows in (B) through (C′) point to abnormal proliferating cells in the SVZ. LV, lateral ventricle.

(D) The H&E-stained sections from similar areas of control brain (a–c) and the proliferating cluster of Mut-1 brain (d–f) were imaged and shown at three different magnifications.

(E) Adjacent sections of the control and Mut-1 brains (D) were stained with anti-Nestin and anti-p53 antibodies.

(F and G) Similar morphological and immunohistochemical analyses of (D and E) were performed on control brain and a proliferating cluster of Mut-2 brain. Arrows in (D) and (F) point to abnormal cells with atypical nuclei in mutant brains. Arrows in (E) and (G) point to Nestin$^+$ and p53$^+$ cells in mutant brains. Asterisk in (D) to (G) denotes the lateral ventricle. The dashed lines in (D) and (E) and in (F) mark the border of the SVZ and corpus callosum and the border of the corpus callosum and surrounding tissues, respectively. Ctx, cerebral cortex; CC, corpus callosum; Hp, hippocampus.

(H–K) The sections from the proliferating clusters were stained with anti-p53/anti-Nestin (H) and DAPI (H′); anti-p53/anti-Olig2 (I) and DAPI (I′); anti-Nestin/anti-Olig2 (J) and DAPI (J′); anti-p53/anti-GFAP (K) and DAPI (K′). Arrows in (H)–(K) point to p53$^{\Delta E5\text{-}6}$-positive cells. Arrowheads in (J) and (J′) point to Nestin$^-$/Olig2$^+$ cells that are most likely normal glial progenitors or oligodendrocytes. Arrowheads in (K) and (K′) point to the p53-negative nuclei of GFAP$^+$ cells. The inset in (H) shows atypical nuclei of two p53$^+$/Nestin$^+$ cells (arrowheads). Scale bars, 25 μm.

Given that a detectable level of mutant p53$^{\Delta E5\text{-}6}$ proteins is exclusively identified in advanced-stage malignant glioma cells, we then sought to determine whether the expression of mutant p53$^{\Delta E5\text{-}6}$ proteins can specifically mark glioma precursors. We found that about 90% of the proliferating cells revealed by BrdU staining in the corpus callosum expressed a detectable level of mutant p53$^{\Delta E5\text{-}6}$ proteins whereas no cells exhibited such expression in the similar areas of normal brains (Figures 5E and 5G, bottom panels). Double-immunofluorescence labeling revealed that Nestin and mutant p53$^{\Delta E5\text{-}6}$ proteins were almost always coexpressed in these cells (Figures 5H and 5H′). Furthermore, the p53$^{\Delta E5\text{-}6}$-positive cells expressed Olig2, but not GFAP, CD133, or markers for lineage-restricted progenitors such as PSA-NCAM (a SVZ-A cell marker) or NG2 (a SVZ-OPC cell marker) (Figures 5I, 5I′, 5K, and 5K′ and data not shown). We further confirmed that all the Nestin$^+$ cells in the proliferating clusters coexpressed Olig2 (Nestin$^+$/Olig2$^+$, Figures 5J and 5J′), demonstrating that glioma precursors are distinct from Nestin$^-$/Olig2$^+$ normal glial progenitors or oligodendrocytes in the corpus callosum (Figures 5J and 5J′, arrowheads). Taken together, these results demonstrate that the expression of mutant p53$^{\Delta E5\text{-}6}$ proteins specifically marks glioma precursors, which immunohistochemically resemble a subpopulation of transit-amplifying SVZ-C progenitor cells (hereafter, SVZ-C*) with the lineage marker expression pattern of Nestin$^+$/GFAP$^-$/Olig2$^+$/CD133$^-$.

To validate that the initially expanded p53$^{\Delta E5\text{-}6}$-positive SVZ-C*-like cells are glioma precursors, we analyzed 19 grossly healthy p53$^{\Delta E5\text{-}6}$ mice at older ages (6 to 9 months) along with 3 mutant mice with non-CNS sarcomas at 10 to 12 months of age. Of these 22 grossly normal p53$^{\Delta E5\text{-}6}$ brains, 15 exhibited no microscopically visible tumor mass (Table S3). Compared to the mutant brains at younger ages, all the brains with no microscopically visible tumor (n = 14) analyzed between the ages of 6 and 10 months had markedly increased numbers of p53$^{\Delta E5\text{-}6}$-positive cells in the corpus callosum and adjacent areas, indicating a continuous expansion of the p53$^{\Delta E5\text{-}6}$-positive cellular populations during tumor development (Figure S8). In all but 2 of these 14 mutant brains, the p53$^{\Delta E5\text{-}6}$-positive cells were specifically distributed in the forebrain areas that are anatomically immediately adjacent to the SVZ-associated areas (Table S3 and Figure S8). Importantly, most, if not all, of the continuously expanded p53$^{\Delta E5\text{-}6}$-positive cells exhibited the similar features of glioma precursors identified in younger mutant mice, which include hyperproliferation and expression of Nestin and Olig2, but not GFAP (Figure S8 and data not shown). Together, these results suggest that the p53$^{\Delta E5\text{-}6}$-positive SVZ-C*-like cells in

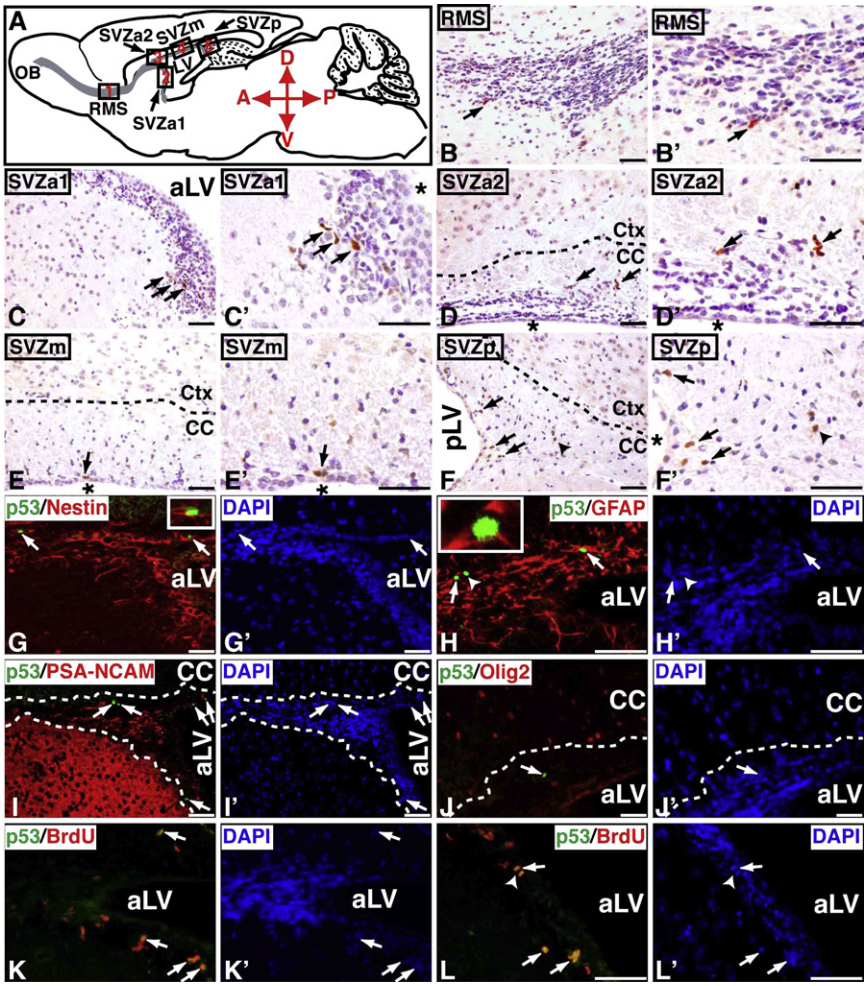


**Figure 6. A Minor Population of SVZ Stem and Progenitor Cells Exhibits a Detectable Mutant $p53^{\Delta E5-6}$ Protein Expression in Young Adult Brain**

(A) Schematic drawing of the sagittal plane of the adult mouse brain. Except for the dentate gyrus of the hippocampus, all the Nestin$^{+}$ cells in the adult brain are restrictively located in the SVZ and RMS and colored in gray. Different parts of the RMS and SVZ are shown in five designated boxed areas. At 2 months of age, most of the $p53^{\Delta E5-6}$-positive cells (B to F′, arrows) are identified in the adult neurogenic areas, which include the RMS (B and B′), the anterior SVZ (C and C′, SVZa1; and D and D′, SVZa2), medial SVZ (E and E′, SVZm), and posterior SVZ (F and F′, SVZp). The arrowhead in (F) and (F′) points to a $p53^{\Delta E5-6}$-positive cell in the adjacent corpus callosum. Sections of the anterior SVZ from 2-month-old $p53^{\Delta E5-6}$ mice were stained by anti-p53/anti-Nestin (G) and DAPI (G′); anti-p53/anti-GFAP (H) and DAPI (H′); anti-p53/anti-PSA-NCAM (I) and DAPI (I′); anti-p53/anti-Olig2 (J) and DAPI (J′); and anti-p53/anti-BrdU (K and L) and DAPI (K′ and L′). Arrows in (G)–(L′) point to the $p53^{\Delta E5-6}$-positive cells in the SVZ. An arrowhead in (H) and (H′) points to a $p53^{\Delta E5-6}$-positive/GFAP-negative progenitor cell. The insets in (G) and (H) show the high-magnification views of the $p53^{\Delta E5-6}$-positive cells expressing Nestin and GFAP, respectively. Arrowheads in (L) and (L′) point to a $p53^{\Delta E5-6}$-positive cells during mitosis. aLV and pLV, anterior and posterior lateral ventricle; (*), lateral ventricle. Scale bars, 25 μm.

the corpus callosum are glioma precursors, whose continuous expansion underlies malignant glioma development. These observations also demonstrate that the histologically homogeneous $p53^{\Delta E5-6}$-positive SVZ-C*-like glioma precursors can give rise to malignant gliomas with a high degree of heterogeneity.

## A Minor Population of Adult SVZ Cells Express Mutant $p53^{\Delta E5-6}$ Proteins

The observations described above raise the possibility that we might be able to identify the cell of origin for $p53^{\Delta E5-6}$-positive malignant glioma cells by determining which cell type in mutant brains first accumulates a detectable level of mutant $p53^{\Delta E5-6}$ proteins. To test this, we analyzed the brain of 11 2-month-old $p53^{\Delta E5-6}$ mice when there was no overt abnormality. Immunohistochemical analysis revealed that 1 of these 11 mutant brains lacked any $p53^{\Delta E5-6}$-positive cells and 5 of them exhibited p53 expression only in one of the two brain hemispheres. These results further confirm the notion that accumulation of a detectable $p53^{\Delta E5-6}$ protein expression is not an inherent property of this mutant allele, but rather a tumor-dependent event and hence may be used for identifying incipient tumor cells.

In the brains with $p53^{\Delta E5-6}$ expression, about 80% of $p53^{\Delta E5-6}$-positive cells were exclusively identified in the adult SVZ niche, including the anterior (SVZa1 and SVZa2), medial (SVZm), and posterior SVZ (Figures 6A and 6C–6F′). Approximately 14% of $p53^{\Delta E5-6}$-positive cells were found in the RMS (Figures 6B and B′), and a minor population was identified in the areas of the corpus callosum just outside the SVZ (Figures 6F and 6F′, arrowhead). Similar to the SVZ-B stem cells, all the $p53^{\Delta E5-6}$-positive cells expressed Nestin and about 90% of those expressed GFAP, but not markers for lineage-restricted cells (e.g., PSA-NCAM and Olig2) (Figures 6G–6J′) (Merkle and Alvarez-Buylla, 2006; Stiles and Rowitch, 2008). A small population of the $p53^{\Delta E5-6}$-positive cells in the SVZ were GFAP negative, which resemble the transit-amplifying SVZ-C progenitor cells (Figures 6H and 6H′, arrowhead) (Merkle and Alvarez-Buylla, 2006). Together, these results suggest that a minor population of the adult SVZ cells, particularly the SVZ-B stem cells with the lineage marker expression pattern of Nestin$^{+}$/GFAP$^{+}$/PSA-NCAM$^{-}$/Olig2$^{-}$/NG2$^{-}$/CD133$^{-}$, are the first and the primary cell types that accumulate a detectable $p53^{\Delta E5-6}$ protein expression in the young adult brain. However, it is worth noting that these $p53^{\Delta E5-6}$-positive cells morphologically were not significantly different from the surrounding SVZ cells (Figure 6).

To assess whether these $p53^{\Delta E5-6}$-positive SVZ cells manifested other tumor cell characteristics, we examined the percentage of proliferating cells in the $p53^{\Delta E5-6}$-positive and -negative cellular compartments. As revealed by BrdU staining,

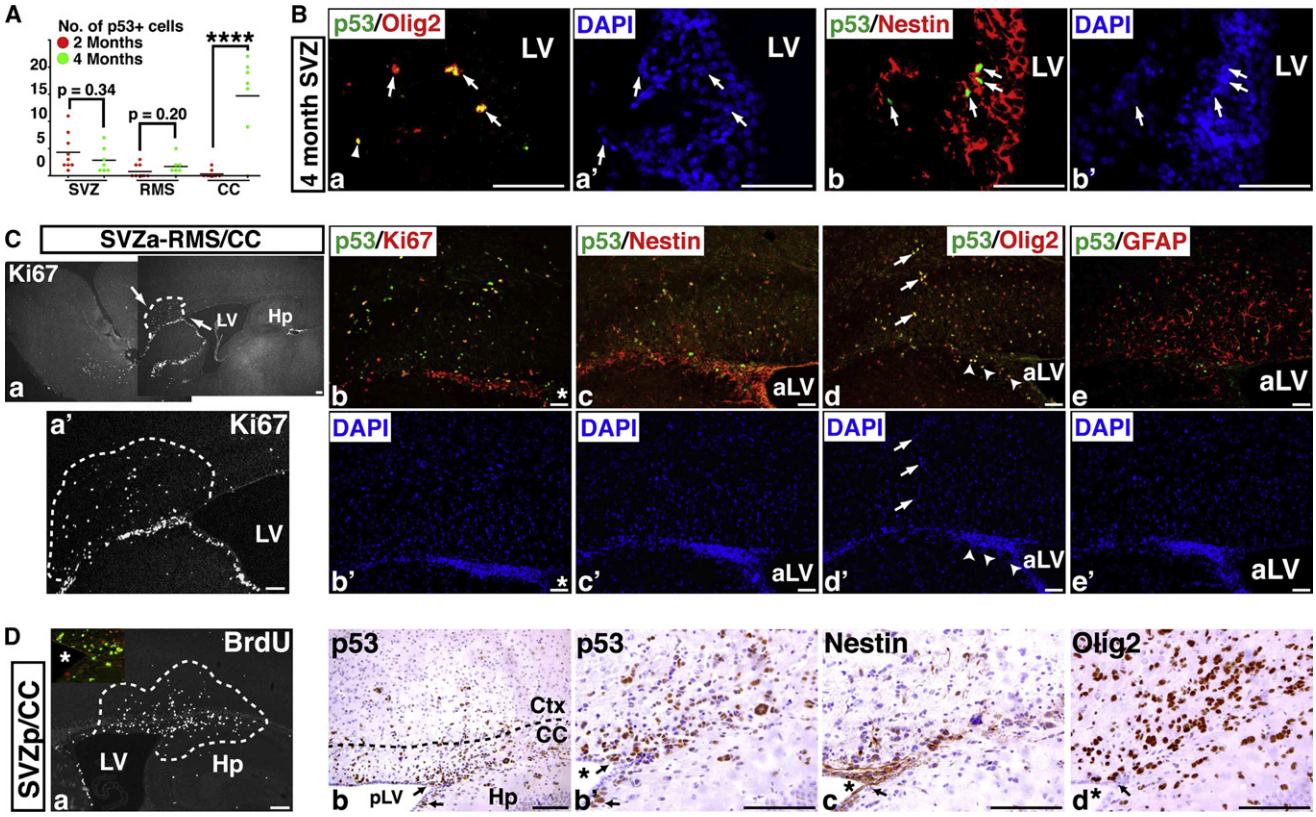


**Figure 7. A Possible Lineage Relationship between p53$^{\Delta E5\text{-}6}$-Positive SVZ-B Stem Cells and SVZ-C* Progenitor-like Glioma Precursors**

(A) The quantification of p53$^{\Delta E5\text{-}6}$-positive cells in brains of mutant mice at 2 and 4 months. Each dot represents the quantification from each individual brain. ****$p < 0.0001$.

(B) Sections from a 4-month-old mutant brain were stained with anti-p53/anti-Olig2 (a) and DAPI (a′) and anti-p53/anti-Nestin (b) and DAPI (b′), in which arrows point to p53$^{\Delta E5\text{-}6}$-positive cells in the SVZ.

(C) One representative mutant brain has proliferating clusters (marked by dashed lines) in the corpus callosum directly associated with the anterior SVZ (a and a′). Sections from this proliferating cluster were stained with anti-p53/anti-Ki67 (b) and DAPI (b′); anti-p53/anti-Nestin (c) and DAPI (c′); anti-p53/anti-Olig2 (d) and DAPI (d′); and anti-p53/anti-GFAP (e) and DAPI (e′). Arrows and arrowheads in (d) and (d′) point to p53$^{\Delta E5\text{-}6}$-positive Olig2$^{+}$ SVZ-C*-like glioma precursors located in the corpus callosum and SVZ, respectively.

(D) Adjacent sections from one proliferating cluster identified in the posterior SVZ (a) were stained with anti-p53 (b and b′), anti-Nestin (c), and anti-Olig2 antibodies (d). Arrows in (b) to (d) point to p53$^{\Delta E5\text{-}6}$-positive glioma precursors inside the SVZ. The inset in (a) shows the high-magnification view of proliferating p53$^{\Delta E5\text{-}6}$-positive glioma precursors in the SVZ (BrdU[green]/p53[red]). aLV and pLV, anterior and posterior lateral ventricle; *, lateral ventricle. Scale bars: (Ca, Ca′, and Da) 100 μm ; (B, Cb–Ce′, and Db–Dd) 50 μm.

about 33% of the p53$^{\Delta E5\text{-}6}$-negative stem or progenitor cells were proliferating in the mutant SVZ (370/1112, n = 4 brains). Strikingly, nearly 77% of the p53$^{\Delta E5\text{-}6}$-positive SVZ cells were proliferating (36/47; n = 7 brains; p53$^{high}$ versus p53$^{negative}$; $p < 0.0001$) (Figures 6K–6L′). Because most of the p53$^{\Delta E5\text{-}6}$-positive cells were immunohistochemically identified as SVZ-B stem cells that are relatively a quiescent cell population (Merkle and Alvarez-Buylla, 2006), these results suggest that the expression of mutant p53$^{\Delta E5\text{-}6}$ proteins may identify a subpopulation of SVZ stem cells as incipient tumor cells in otherwise relatively normal brains at this age.

## A Possible Lineage Relationship between p53$^{\Delta E5\text{-}6}$-Positive Cell Populations

The hyperproliferative phenotypes of p53$^{\Delta E5\text{-}6}$-positive SVZ-B stem cells in the 2-month-old brain raise the possibility that these cells are the cell of origin for the p53$^{\Delta E5\text{-}6}$-positive SVZ-C*-like glioma precursors identified in the corpus callosum of the older mice. To study a possible lineage relationship between these two p53$^{\Delta E5\text{-}6}$-positive cell populations, we quantified the number of p53$^{\Delta E5\text{-}6}$-positive cells in mutant brains at these two ages. Except for the corpus callosum, the number of p53$^{\Delta E5\text{-}6}$-positive cells in mutant SVZ or RMS at 4 months was not significantly increased compared to those at a younger age (Figure 7A). However, in contrast to the p53$^{\Delta E5\text{-}6}$-positive cells that rarely expressed Olig2 in the 2-month-old SVZ, over 60% of the p53$^{\Delta E5\text{-}6}$-positive cells in the SVZ and RMS at 4 months acquired Olig2 expression and exhibited the same lineage marker expression pattern as that of the p53$^{\Delta E5\text{-}6}$-positive glioma precursors (Figure 7B). These results suggest that similar to normal stem cells, the p53$^{\Delta E5\text{-}6}$-positive SVZ-B stem cells can differentiate into Olig2$^{+}$ SVZ-C* progenitor cells, which may function as an intermediate cell type between SVZ-B stem cells and Olig2$^{+}$ SVZ-C*-like glioma precursors. In support of such a transition,

most of the proliferating clusters were identified in the areas immediately adjacent to the adult SVZ neurogenic niches, some of which directly involved the cells in the SVZ (Figures 7C and 7D). More importantly, within these proliferating clusters, the $p53^{\Delta E5\text{-}6}$-positive cells inside and outside the SVZ stem cell niche expressed the same lineage markers as the $Olig2^+$ SVZ-C* progenitors regardless of the positions at the anterior SVZ (Figure 7C and Figure S9) or posterior SVZ (Figure 7D).

If the $p53^{\Delta E5\text{-}6}$-positive SVZ-B stem cells give rise to the $p53^{\Delta E5\text{-}6}$-positive $Olig2^+$ SVZ-C*-like glioma precursors, both should be p53 deficient and thus can be labeled by Cre-mediated R26R-LacZ expression. To test this, we studied the R26R-LacZ expression in the $p53^{\Delta E5\text{-}6}$ brain. In contrast to most mature astrocytes, all the $p53^{\Delta E5\text{-}6}$-positive SVZ cells expressed β-gal in the mutant brains at 2 months, confirming our lineage marker analysis that these cells were SVZ stem cells or transit-amplifying progenitors (Figure 8A). Furthermore, all the $p53^{\Delta E5\text{-}6}$-positive glioma precursors could also be identified by β-gal expression within the proliferating clusters located in the corpus callosum of older mutant brains (Figures 8B and 8C). These results indicate that both $p53^{\Delta E5\text{-}6}$-positive SVZ-B stem cells and $Olig2^+$ SVZ-C*-like glioma precursors are p53 deficient, supporting the notion that these neural stem and progenitor-like cells are the precursors for p53-deficient malignant glioma cells in this model. Finally, of the mutant brains identified with a proliferating cluster, one rare case contained $p53^{\Delta E5\text{-}6}$-positive glioma precursors in the neuronal layers of the OB (Figures 8Da and 8Da′). Despite their presence in the migratory destination of neuroblasts, these $p53^{\Delta E5\text{-}6}$-positive glioma precursors expressed the same lineage markers as $Olig2^+$ SVZ-C* progenitors (Figures 8Db–8Dd). Thus, these observations indicate that some glioma precursors exhibit the cellular characteristics of migrating neuroblasts, another progeny of multipotent SVZ neural stem cells.

## DISCUSSION

### A Central Role of p53 Deficiency in Gliomagenesis

This study demonstrates that a single *p53* mutation can efficiently induce malignant astrocytic glioma formation in mice. In contrast, using the same hGFAP-cre driver as described here, we previously showed that the hGFAP-cre+;$Nf1^{flox/flox}$ mice exhibited no evidence of tumor formation in the brain, even in the *p53* heterozygous background, despite *Nf1*-deficient brain cells having activation of both MAPK and PI3K/Akt signaling pathways (Zhu et al., 2005a, 2005b). However, *p53* deficiency can cooperate with *Nf1* or *Pten* heterozygous mutations to efficiently induce malignant astrocytic gliomas in mice (Reilly et al., 2000; Zheng et al., 2008; Zhu et al., 2005a). These results reveal a central role of p53 deficiency in gliomagenesis. Surprisingly, analysis of brains of mutant mice at younger ages reveals that p53 deficiency provides no significant growth advantage to brain cells but rather appears to induce pleiotropic accumulation of cooperative oncogenic alterations in Rb and RTK pathways. One intriguing finding of this study is that a sizable fraction of $p53^{\Delta E5\text{-}6}$ gliomas exhibited no activation of MAPK (~50%) or PI3K/Akt (~20%) pathways. Furthermore, the majority of the $p53^{\Delta E5\text{-}6}$ gliomas exhibited increased instead of decreased levels of Nf1 protein expression. Similar results were also observed in human GBMs (Gutmann et al., 1996; Mawrin et al., 2003; Wang et al., 2004). Together, these observations demonstrate that p53-deficient brain cells are highly plastic with abilities to cooperate with diverse downstream oncogenic alterations to drive glioma development (Figure 8E) and raise the concern of whether inhibitors for the MAPK and PI3K/AKT pathways will be effective to treat human GBM.

### Cell of Origin for Malignant Astrocytic Glioma

Murine models have been widely used to study the cell-of-origin of a cancer. Ideally, an oncogenic mutation can be targeted into the cells at various developmental stages of a specific cell lineage. However, this approach is often limited in the CNS due to a lack of well-defined cell lineage-specific promoters. For example, despite being one of the best characterized and the most widely used CNS stem/progenitor cell marker, Nestin is expressed not only in multipotent SVZ-B neural stem cells and SVZ-C transit-amplifying progenitors but also in lineage-restricted SVZ-A neuroblasts in the adult brain (Doetsch et al., 1997). Moreover, if a deletion-based mutational strategy (e.g., Cre/loxP system) is employed to drive tumor formation, lineage-restricted SVZ-OPC glial progenitors and oligodendrocytes, albeit expressing no Nestin, will inherit the same mutations that are targeted in $Nestin^+$ SVZ-B and C cells (Menn et al., 2006). Thus, with currently available technologies, it is not feasible to specifically target a genetic mutation in the multipotent CNS stem/progenitor cells.

Compared to currently available p53-associated glioma models, one feature of our model is that mutant $p53^{\Delta E5\text{-}6}$ proteins are accumulated to a detectable level in all stages of glioma cells but not in normal brain cells. Combining with proliferation, lineage marker expression, and morphological analysis, we used this p53 marker to study glioma precursors at the single-cell level during the earliest stages of tumor development. Although advanced-stage $p53^{\Delta E5\text{-}6}$ gliomas are extremely heterogeneous histopathologically and molecularly, the $p53^{\Delta E5\text{-}6}$-positive glioma precursors are remarkably homogeneous and exhibit a lineage marker expression pattern reminiscent of $Olig2^+$ SVZ-C* transit-amplifying progenitor cells. Moreover, despite that the $p53^{\Delta E5\text{-}6}$ mutation was targeted to diverse CNS cell populations throughout the brain, the $p53^{\Delta E5\text{-}6}$-positive glioma precursors were exclusively identified in the two brain areas, corpus callosum and OB, which are the migratory destinations of the two differentiated progeny of the multipotent SVZ stem cells. Therefore, the lineage marker expression pattern and anatomical location of glioma precursors suggest that the $p53^{\Delta E5\text{-}6}$-positive malignant glioma cells may arise from multipotent SVZ stem cells and/or transit-amplifying progenitors. Consistently, we demonstrate that the SVZ-B stem cells and SVZ-C progenitors are the earliest cell types that accumulate a detectable $p53^{\Delta E5\text{-}6}$ protein expression in the brain of younger mutant mice. Based on these results, we propose a model for the role of neural stem cells and transit-amplifying progenitors in p53-mediated gliomagenesis: (1) the SVZ-B stem cells are most susceptible to accumulation of oncogenic alterations, as evidenced by high levels of mutant $p53^{\Delta E5\text{-}6}$ expression; (2) the glioma-initiating cells are the $Olig2^+$ SVZ-C* progenitor-like cells at the earliest stages of tumor development; (3) the majority of differentiation-stalled $Olig2^+$ SVZ-C* progenitor-like cells migrate as SVZ-OPCs to the corpus callosum and a minor population migrate as SVZ-A neuroblasts to the RMS and OB; (4) $p53^{\Delta E5\text{-}6}$-positive SVZ-C*-like glioma

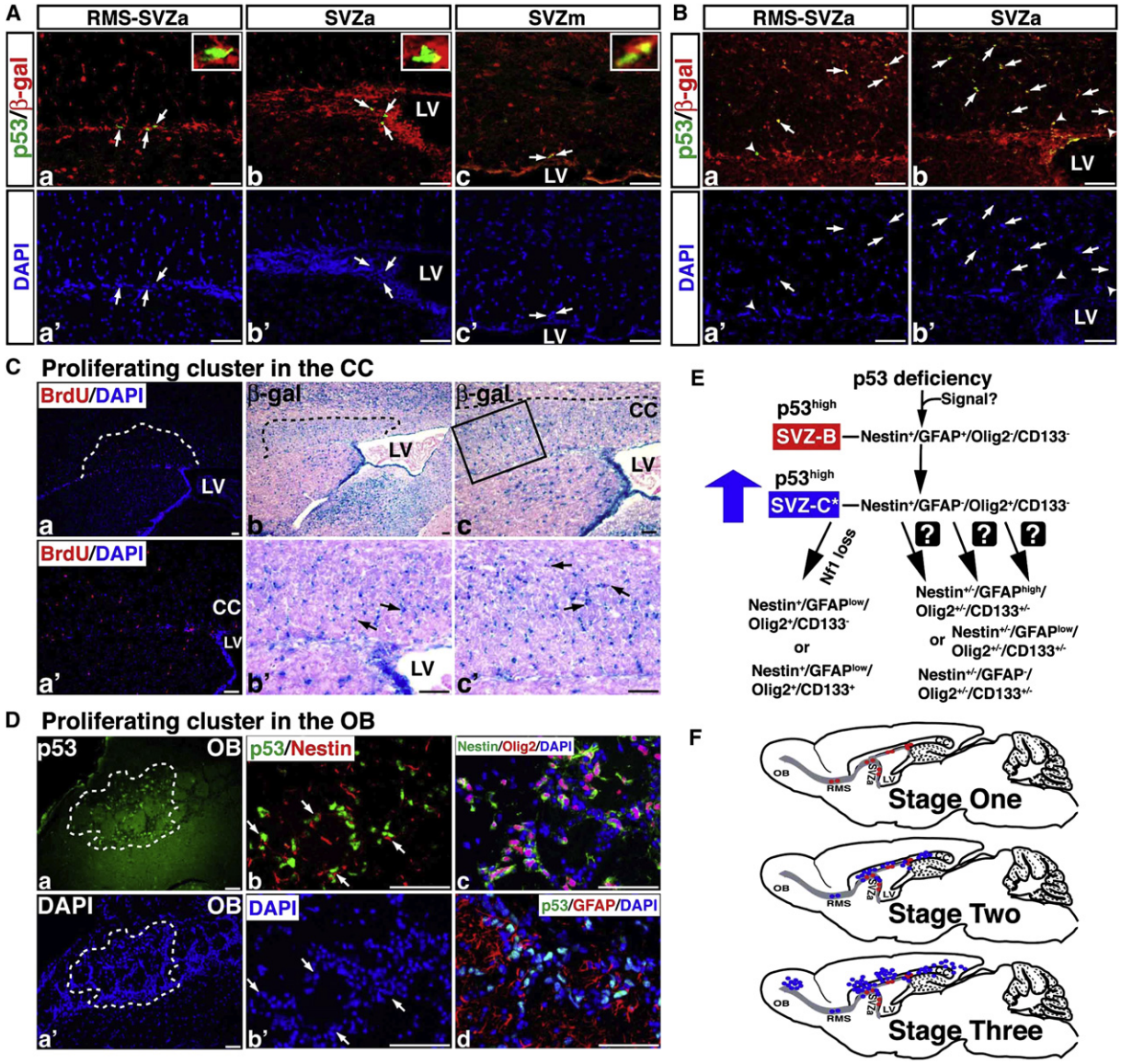


**Figure 8. p53$^{\Delta E5\text{-}6}$-Positive SVZ Stem Cells and Glioma Precursors Express the R26R-LacZ**

(A) Sections from 2-month-old p53$^{\Delta E5\text{-}6}$ brains with the R26R-LacZ transgene were stained with anti-p53/anti-β-gal antibodies (a–c) and were counterstained with DAPI for labeling nuclei (a′–c′). All the p53$^{\Delta E5\text{-}6}$-positive cells (arrows) at this age express β-gal of the R26R-LacZ regardless of their location in the RMS or anterior or medial SVZ (SVZa and SVZm). The insets in (a)–(c) show the high-magnification views of p53/β-gal double-positive cells.

(B) Two representative proliferating clusters identified in the corpus callosum adjacent to either the junction of RMS and SVZa (a and a′) or SVZa (b and b′) were sectioned and stained with anti-p53/anti-β-gal antibodies. Within these proliferating clusters, all the p53$^{\Delta E5\text{-}6}$-positive glioma precursors in the corpus callosum (arrows) and SVZ (arrowheads) express β-gal of the R26R-LacZ.

(C) Adjacent sections of a proliferating cluster were stained by BrdU/DAPI staining (a and a′) and X-gal (b and c). (b′ and c′) High-magnification views of the boxed areas shown in (b) and (c) reveal a group of β-gal-positive cells with atypical nuclei (arrows). LV, lateral ventricle.

(D) A mutant brain contains p53$^{\Delta E5\text{-}6}$-positive glioma precursors in the OB (a and a′). Sections from this proliferating cluster were stained with anti-p53/anti-Nestin (b) and DAPI (b′), anti-Nestin/anti-Olig2/DAPI (c), and anti-p53/anti-GFAP/DAPI (d). Arrows in (b) and (b′) point to p53$^{\Delta E5\text{-}6}$-positive cells.

(E) A model summarizes p53-mediated gliomagenesis (see Discussion for details).

(F) The anatomical location of p53$^{\Delta E5\text{-}6}$-positive early-stage glioma precursors during tumor development. Red dots, p53$^{\Delta E5\text{-}6}$-positive SVZ-B stem cells; blue dots, p53$^{\Delta E5\text{-}6}$-positive SVZ-C*-like glioma precursors. Scale bars, 50 μm.

precursors can use diverse cooperative oncogenic alterations to form high-grade gliomas with a markedly high degree of heterogeneity (Figures 8E and 8F).

Although the expression of mutant p53 proteins provides a sensitive tool to monitor early-stage glioma cells at the single-cell level, the extremely low number of the p53$^{\Delta E5\text{-}6}$-positive cells in mutant brains makes it difficult to establish a definitive lineage relationship between the morphologically normal p53$^{\Delta E5\text{-}6}$-positive neural stem cells and glioma precursors. However, we obtain several independent lines of evidence supporting

a lineage relationship between these two $p53^{\Delta E5\text{-}6}$-positive cell populations. First, $p53^{\Delta E5\text{-}6}$-positive cells in the SVZ are the only cells that exhibit measurable tumor cell characteristics, such as hyperproliferation, suggesting that these cells are the incipient glioma cells in otherwise normal brains at 2 months. Second, we identify an intermediate cell type between $p53^{\Delta E5\text{-}6}$-positive SVZ-B stem cells and $Olig2^+$ SVZ-C*-like glioma precursors in the 4-month-old mutant brains. These $p53^{\Delta E5\text{-}6}$-positive intermediate cells resemble $Olig2^+$ SVZ-C*-like glioma precursors, but are located in the SVZ. Consistently, in some proliferating clusters, expansion of the $p53^{\Delta E5\text{-}6}$-positive SVZ-C*-like glioma precursors can be found in both the SVZ and corpus callosum. Finally, both $p53^{\Delta E5\text{-}6}$-positive SVZ-B stem cells and $Olig2^+$ SVZ-C*-like glioma precursors in the corpus callosum can be marked by Cre-mediated R26R-LacZ expression, indicating that these two cell populations are genetically p53 deficient.

## Murine GBM Models and Clinical Implication

Malignant astrocytic gliomas observed in the $p53^{\Delta E5\text{-}6}$ model recapitulate genetic, histopathological, and molecular features of human GBM (Furnari et al., 2007; Louis et al., 2007). The utility of the $p53^{\Delta E5\text{-}6}$ model is further illustrated by the cooperation of the $p53^{\Delta E5\text{-}6}$ mutation with an *Nf1* heterozygous mutation, which produces a fast-growing GBM model, albeit at the expense of loss of histopathological and molecular heterogeneity. These results suggest that cooperative oncogenic alterations influence the histological features of advanced-stage malignant glioma cells, despite arising from remarkably homogeneous progenitor-like cells. Finally, given that the *Nf1* heterozygous mutation has no tumor-inducing activity in the brain, the robust GBM phenotypes observed in the $p53^{\Delta E5\text{-}6}$;$Nf1^{-/-}$ (CKO3) mice indicate that the $p53^{\Delta E5\text{-}6}$ mice provide a sensitive genetic background for glioma development. With the advent of the Cancer Genome Atlas initiative, this important feature will be particularly valuable to validate newly identified glioma genes and to generate a series of GBM models for preclinical testing of therapies that target more specific oncogenic pathways.

## EXPERIMENTAL PROCEDURES

### Control and Conditional CKO1, CKO2, and CKO3 Mutant Mice

The mutant mice that harbor a *p53* null mutation ($p53^{KO}$) (Jacks et al., 1994) and a floxed *p53* allele ($p53^{flox}$) (Lin et al., 2004) were maintained on the 129Svj/C57Bl6 hybrid genetic background. The hGFAP-cre transgenic mice were originally generated on the FVB background (Zhuo et al., 2001) and have subsequently been backcrossed to the 129Svj/C57Bl background for more than five generations (Zhu et al., 2005a). Therefore, CKO1 and CKO2 mice analyzed in this study were maintained on approximately 99% 129Svj/C57Bl6 (49.5%/49.5%) and less than 1% FVB hybrid background. Many CKO1 and CKO2 mice analyzed in this study were littermates. Control mice were the pool of phenotypically indistinguishable mice with genotypes of hGFAP-cre-;$p53^{flox/KO}$ and hGFAP-cre-;$p53^{flox/flox}$. Introduction of an *Nf1* heterozygous mutation (Brannan et al., 1994) to the CKO2 background generated the CKO3 mice, which shared the same genetic background as CKO1 and CKO2 mice. All mice in this study were cared for according to the guidelines that were approved by the Animal Care and Use Committees of the University of Michigan at Ann Arbor.

### Histological Grading of Malignant Astrocytic Gliomas in CKO1, CKO2, and CKO3 Mice

Histopathology of neoplasms that developed in these mice had to meet diagnostic criteria of the World Health Organization for classification of tumors of the CNS (Louis et al., 2007). Tumors with neoplastic astrocyte-like cells were classified as astrocytic gliomas. Astrocytic features include extension of cellular processes from neoplastic cells. These vary from long and thick to thin and short. They are highlighted with H&E and GFAP stains. Variable nuclear shapes, particularly elongated, bent, and dark staining nuclei characterize neoplastic astrocytes. Their perinuclear cytoplasm is highly variable: from imperceptible to substantial and appearing to push the nucleus to the perimeter of the cell. Detailed histopathological grading of these murine malignant astrocytic gliomas is provided in the Supplemental Experimental Procedures.

### Quantification and Statistical Analysis

To quantify the number of immunohistochemically labeled cells, anatomically comparable sections from control and mutant brains were visualized under 40× magnification using an Olympus BX51 microscope. Images were captured and subjected to double-blinded counting. Lengths and areas were measured by the NIH software ImageJ. The number of cells was quantified and statistical analysis was carried out using two-tailed Student's t test. $p < 0.05$ was considered to be statistically significant. To compare the proportions from two independent cell populations and to determine if they are significantly different from one another, the number of specific cell types were quantified and subjected to z test for proportions. These results were also confirmed by chi-square test. $p < 0.05$ was considered to be statistically significant.

### Detection of the $p53^{\Delta E5\text{-}6}$-Positive Cells in the Mutant Brains at Early Stages of Tumor Development

The brain of the $p53^{\Delta E5\text{-}6}$ mice at ages of 2 months, 4 to 4.5 months, and 6 to 9 months were dissected and examined for enlargement under a dissecting microscope. Only the grossly normal mutant brains were used to study glioma cells in early stages. The mutant brains were evenly cut into four pieces along the midline (two pieces for each brain hemisphere) and subsequently were processed for paraffin-embedded sections. Each brain was serially sectioned at sagittal planes and four 5 μm paraffin sections were put on a single slide. At four independent sagittal planes, we sampled a total of 1760 μm brain thickness along the midline to lateral hemisphere for each mutant brain. Serial sections were stained with an anti-p53 antibody and visualized with DAB staining. We examined $p53^{\Delta E5\text{-}6}$-positive cells in these sections under a light microscope (J.Y. and Y.Z.). Once we determined the restricted distribution of $p53^{\Delta E5\text{-}6}$-positive cells in the corpus callosum, SVZ/RMS, and their associated areas of mutant brains, we focused on the brain areas that contain the SVZ and RMS of the lateral ventricle. Double-immunofluorescence labeling was performed on the adjacent sections to determine the identity of the $p53^{\Delta E5\text{-}6}$-positive cells.

### Histological, Molecular, Genetic, and Statistical Analyses

Detailed descriptions for the experimental procedures are provided in the Supplemental Experimental Procedures.

## SUPPLEMENTAL DATA

Supplemental Data contain Supplemental Experimental Procedures, nine figures, and three tables and can be found with this article online at http://www.cell.com/cancer-cell/supplemental/S1535-6108(09)00114-7.

## ACKNOWLEDGMENTS

We thank L. Liu, L. Cregan, M. Best, and M. Hancock for technical assistance; members of the Zhu laboratory for support; Dr. L. Parada for support at early stages of the project; A. Messing for providing hGFAP-cre+ mice; C. Stiles and B. Novitch for Olig2 antibodies; and Drs. E. Fearon, S. Morrison, and L. Chang for comments. This work is supported by grants from the National Institutes of Health (1R01 NS053900), the National Brain Tumor Society, and the Comprehensive Cancer Center and Biological Sciences Scholars Program of the University of Michigan (Y.Z.). Y.Z. is an American Cancer Society research scholar.

Received: October 16, 2008
Revised: January 20, 2009
Accepted: April 1, 2009
Published: June 1, 2009

## REFERENCES

Alcantara Llaguno, S., Chen, J., Kwon, C.H., Jackson, E.L., Li, Y., Burns, D.K., Alvarez-Buylla, A., and Parada, L.F. (2009). Malignant astrocytomas originate from neural stem/progenitor cells in a somatic tumor suppressor mouse model. Cancer Cell *15*, 45–56.

Brannan, C.I., Perkins, A.S., Vogel, K.S., Ratner, N., Nordlund, M.L., Reid, S.W., Buchberg, A.M., Jenkins, N.A., Parada, L.F., and Copeland, N.G. (1994). Targeted disruption of the neurofibromatosis type-1 gene leads to developmental abnormalities in heart and various neural crest-derived tissues. Genes Dev. *8*, 1019–1029.

Calabrese, C., Poppleton, H., Kocak, M., Hogg, T.L., Fuller, C., Hamner, B., Oh, E.Y., Gaber, M.W., Finklestein, D., Allen, M., et al. (2007). A perivascular niche for brain tumor stem cells. Cancer Cell *11*, 69–82.

Cancer Genome Atlas Research Network. (2008). Comprehensive genomic characterization defines human glioblastoma genes and core pathways. Nature *455*, 1061–1068.

Cho, Y., Gorina, S., Jeffrey, P.D., and Pavletich, N.P. (1994). Crystal structure of a p53 tumor suppressor-DNA complex: understanding tumorigenic mutations. Science *265*, 346–355.

Doetsch, F., Garcia-Verdugo, J.M., and Alvarez-Buylla, A. (1997). Cellular composition and three-dimensional organization of the subventricular germinal zone in the adult mammalian brain. J. Neurosci. *17*, 5046–5061.

Donehower, L.A., Harvey, M., Slagle, B.L., McArthur, M.J., Montgomery, C.A., Jr., Butel, J.S., and Bradley, A. (1992). Mice deficient for p53 are developmentally normal but susceptible to spontaneous tumours. Nature *356*, 215–221.

Furnari, F.B., Fenton, T., Bachoo, R.M., Mukasa, A., Stommel, J.M., Stegh, A., Hahn, W.C., Ligon, K.L., Louis, D.N., Brennan, C., et al. (2007). Malignant astrocytic glioma: genetics, biology, and paths to treatment. Genes Dev. *21*, 2683–2710.

Galli, R., Binda, E., Orfanelli, U., Cipelletti, B., Gritti, A., De Vitis, S., Fiocco, R., Foroni, C., Dimeco, F., and Vescovi, A. (2004). Isolation and characterization of tumorigenic, stem-like neural precursors from human glioblastoma. Cancer Res. *64*, 7011–7021.

Gil-Perotin, S., Marin-Husstege, M., Li, J., Soriano-Navarro, M., Zindy, F., Roussel, M.F., Garcia-Verdugo, J.M., and Casaccia-Bonnefil, P. (2006). Loss of p53 induces changes in the behavior of subventricular zone cells: implication for the genesis of glial tumors. J. Neurosci. *26*, 1107–1116.

Gutmann, D.H., Giordano, M.J., Mahadeo, D.K., Lau, N., Silbergeld, D., and Guha, A. (1996). Increased neurofibromatosis 1 gene expression in astrocytic tumors: positive regulation by p21-ras. Oncogene *12*, 2121–2127.

Hack, M.A., Saghatelyan, A., de Chevigny, A., Pfeifer, A., Ashery-Padan, R., Lledo, P.M., and Gotz, M. (2005). Neuronal fate determinants of adult olfactory bulb neurogenesis. Nat. Neurosci. *8*, 865–872.

Hemmati, H.D., Nakano, I., Lazareff, J.A., Masterman-Smith, M., Geschwind, D.H., Bronner-Fraser, M., and Kornblum, H.I. (2003). Cancerous stem cells can arise from pediatric brain tumors. Proc. Natl. Acad. Sci. USA *100*, 15178–15183.

Jacks, T., Remington, L., Williams, B.O., Schmitt, E.M., Halachmi, S., Bronson, R.T., and Weinberg, R.A. (1994). Tumor spectrum analysis in p53-mutant mice. Curr. Biol. *4*, 1–7.

Kitayner, M., Rozenberg, H., Kessler, N., Rabinovich, D., Shaulov, L., Haran, T.E., and Shakked, Z. (2006). Structural basis of DNA recognition by p53 tetramers. Mol. Cell *22*, 741–753.

Lim, D.A., Cha, S., Mayo, M.C., Chen, M.H., Keles, E., VandenBerg, S., and Berger, M.S. (2007). Relationship of glioblastoma multiforme to neural stem cell regions predicts invasive and multifocal tumor phenotype. Neuro-oncol. *9*, 424–429.

Lin, S.C., Lee, K.F., Nikitin, A.Y., Hilsenbeck, S.G., Cardiff, R.D., Li, A., Kang, K.W., Frank, S.A., Lee, W.H., and Lee, E.Y. (2004). Somatic mutation of p53 leads to estrogen receptor alpha-positive and -negative mouse mammary tumors with high frequency of metastasis. Cancer Res. *64*, 3525–3532.

Louis, D.N., Ohgaki, H., Wiestler, O.D., and Cavenee, W.K. (2007). WHO Classification of Tumors of the Central Nervous System (Lyon, France: IARC).

Malatesta, P., Hack, M.A., Hartfuss, E., Kettenmann, H., Klinkert, W., Kirchhoff, F., and Gotz, M. (2003). Neuronal or glial progeny: regional differences in radial glia fate. Neuron *37*, 751–764.

Mawrin, C., Diete, S., Treuheit, T., Kropf, S., Vorwerk, C.K., Boltze, C., Kirches, E., Firsching, R., and Dietzmann, K. (2003). Prognostic relevance of MAPK expression in glioblastoma multiforme. Int. J. Oncol. *23*, 641–648.

Meletis, K., Wirta, V., Hede, S.M., Nister, M., Lundeberg, J., and Frisen, J. (2006). p53 suppresses the self-renewal of adult neural stem cells. Development *133*, 363–369.

Menn, B., Garcia-Verdugo, J.M., Yaschine, C., Gonzalez-Perez, O., Rowitch, D., and Alvarez-Buylla, A. (2006). Origin of oligodendrocytes in the subventricular zone of the adult brain. J. Neurosci. *26*, 7907–7918.

Merkle, F.T., and Alvarez-Buylla, A. (2006). Neural stem cells in mammalian development. Curr. Opin. Cell Biol. *18*, 704–709.

Ohgaki, H., Dessen, P., Jourde, B., Horstmann, S., Nishikawa, T., Di Patre, P.L., Burkhard, C., Schuler, D., Probst-Hensch, N.M., Maiorka, P.C., et al. (2004). Genetic pathways to glioblastoma: a population-based study. Cancer Res. *64*, 6892–6899.

Parsons, D.W., Jones, S., Zhang, X., Lin, J.C., Leary, R.J., Angenendt, P., Mankoo, P., Carter, H., Siu, I.M., Gallia, G.L., et al. (2008). An integrated genomic analysis of human glioblastoma multiforme. Science *321*, 1807–1812.

Reilly, K.M., Loisel, D.A., Bronson, R.T., McLaughlin, M.E., and Jacks, T. (2000). Nf1;Trp53 mutant mice develop glioblastoma with evidence of strain-specific effects. Nat. Genet. *26*, 109–113.

Sanai, N., Alvarez-Buylla, A., and Berger, M.S. (2005). Neural stem cells and the origin of gliomas. N. Engl. J. Med. *353*, 811–822.

Singh, S.K., Hawkins, C., Clarke, I.D., Squire, J.A., Bayani, J., Hide, T., Henkelman, R.M., Cusimano, M.D., and Dirks, P.B. (2004). Identification of human brain tumour initiating cells. Nature *432*, 396–401.

Soriano, P. (1999). Generalized lacZ expression with the ROSA26 Cre reporter strain. Nat. Genet. *21*, 70–71.

Stiles, C.D., and Rowitch, D.H. (2008). Glioma stem cells: a midterm exam. Neuron *58*, 832–846.

Wang, H., Wang, H., Zhang, W., Huang, H.J., Liao, W.S., and Fuller, G.N. (2004). Analysis of the activation status of Akt, NFkappaB, and Stat3 in human diffuse gliomas. Lab. Invest. *84*, 941–951.

Zheng, H., Ying, H., Yan, H., Kimmelman, A.C., Hiller, D.J., Chen, A.J., Perry, S.R., Tonon, G., Chu, G.C., Ding, Z., et al. (2008). p53 and Pten control neural and glioma stem/progenitor cell renewal and differentiation. Nature *455*, 1129–1133.

Zhu, Y., Guignard, F., Zhao, D., Liu, L., Burns, D.K., Mason, R.P., Messing, A., and Parada, L.F. (2005a). Early inactivation of p53 tumor suppressor gene cooperating with NF1 loss induces malignant astrocytoma. Cancer Cell *8*, 119–130.

Zhu, Y., Harada, T., Liu, L., Lush, M.E., Guignard, F., Harada, C., Burns, D.K., Bajenaru, M.L., Gutmann, D.H., and Parada, L.F. (2005b). Inactivation of NF1 in CNS causes increased glial progenitor proliferation and optic glioma formation. Development *132*, 5577–5588.

Zhuo, L., Theis, M., Alvarez-Maya, I., Brenner, M., Willecke, K., and Messing, A. (2001). hGFAP-cre transgenic mice for manipulation of glial and neuronal function in vivo. Genesis *31*, 85–94.